

# Influence of landscape aggregation in modelling snow-cover ablation and snowmelt runoff in a sub-arctic mountainous environment

PABLO F. DORNES<sup>1</sup>, JOHN W. POMEROY<sup>1</sup>, ALAIN PIETRONIRO<sup>2</sup>,  
SEAN K. CAREY<sup>3</sup> & WILLIAM L. QUINTON<sup>4</sup>

<sup>1</sup> Centre for Hydrology, University of Saskatchewan, 117 Science Place, Saskatoon, Saskatchewan S7N 5C8, Canada  
pablo.dornes@usask.ca

<sup>2</sup> National Water Research Institute, Saskatoon, Saskatchewan S7N 3H5, Canada

<sup>3</sup> Geography and Environmental Studies, Carleton University, Ottawa, Ontario K1S 5B6, Canada

<sup>4</sup> Cold Regions Research Centre, Wilfrid Laurier University, Waterloo, Ontario N2L 3C5, Canada

**Abstract** Appropriate representation of landscape heterogeneity at small to medium scales is a central issue for hydrological modelling. Two main hydrological modelling approaches, deductive and inductive, are generally applied. Here, snow-cover ablation and basin snowmelt runoff are evaluated using a combined modelling approach that includes the incorporation of detailed process understanding along with information gained from observations of basin-wide streamflow phenomena. The study site is Granger Basin, a small sub-arctic basin in the mountains of the Yukon Territory, Canada. The analysis is based on the comparison between basin-aggregated and distributed landscape representations. Results show that the distributed model based on “hydrological response” landscape units best describes the observed magnitudes of both snow-cover ablation and basin runoff, whereas the aggregated approach fails to represent the differential snowmelt rates and to describe both runoff volumes and dynamics when discontinuous snowmelt events occur.

**Key words** snowmelt; runoff; HRU; inductive modelling; deductive modelling; aggregation; Yukon Territory

## Influence de l'agrégation paysagère dans la modélisation de l'ablation du couvert neigeux et de l'écoulement de fonte nivale dans un environnement montagneux sub-arctique

**Résumé** Une représentation appropriée de l'hétérogénéité du paysage aux échelles petites à moyennes est une question centrale pour la modélisation hydrologique. Deux approches majeures de modélisation hydrologique, déductive et inductive, sont appliquées. Ici, l'ablation du couvert neigeux et l'écoulement de fonte nivale sont évalués à l'aide d'une approche de modélisation combinée qui incorpore une compréhension détaillée de processus ainsi que des informations déduites d'observations d'écoulement au niveau du bassin versant. Le site d'étude est le bassin versant de Granger, un petit bassin sub-arctique des montagnes du Territoire du Yukon, Canada. L'analyse est basée sur la comparaison entre représentations du paysage agrégée au niveau du bassin versant et distribuée. Les résultats montrent que le modèle distribué basé sur la ‘réponse hydrologique’ d'unités paysagères décrit le mieux les intensités de l'ablation du couvert neigeux et de l'écoulement de bassin, tandis que l'approche agrégée échoue à représenter les taux différentiels de fonte nivale et à décrire les volumes et les dynamiques d'écoulement lors de l'occurrence d'événements de fonte discontinus.

**Mots clefs** fonte nivale; écoulement; HRU; modélisation inductive; modélisation déductive; agrégation; Territoire du Yukon

## INTRODUCTION

A major limitation for hydrological predictions is the quantification of the different uncertainties associated with the representation of model inputs, process descriptions and model parameters, (Sivapalan *et al.*, 2003a). Catchment models are usually conceptualised based on different aggregation approaches and are therefore simplified representations of the real world (Blöschl & Sivapalan, 1995; Wagener, 2003). At small to medium scales (approx. <200 km<sup>2</sup>), reliable hydrological modelling is very difficult because rare or specific features (e.g. macropore distributions, variations of saturated hydraulic conductivity with depth, canopy influences on snowmelt rates) often dominate the hydrological response. Therefore, at these scales, models require incorporation of both detailed process understanding and inputs, along with information gained from observations of basin-wide streamflow phenomena; essentially a combination of deductive or bottom-up and inductive or top-down modelling approaches.

Snowmelt and subsequent infiltration to frozen soils and runoff generation are amongst the most important hydrological processes in arctic and sub-arctic mountain environments. Hillslopes, valley bottoms and plateaus dominate the physiography of these regions in Canada, and both vertical and lateral water fluxes exhibit large variability, since topography, microclimate, soil properties, frost and vegetation vary widely over short distances (Carey & Woo, 2001). The influence of slope and aspect are very important for hillslope snowmelt calculations, because they affect snow accumulation, snowmelt energetics, resulting meltwater fluxes and runoff contributing area (Carey & Woo, 1998). Pomeroy *et al.* (2003) found substantial differences in energetics and rates of snow ablation over shrub-tundra surfaces of varying slope and aspect. They found that differences in solar radiation on north-facing (NF) and south-facing (SF) slopes initially caused small differences in net radiation in early melt. However, as shrubs and bare ground emerged due to faster melting on the SF slope, the albedo differences resulted in large positive values of net radiation to the SF, whilst the NF fluxes remained negative. Pomeroy *et al.* (2006) showed the importance of shrub exposure in governing snowmelt energy; in general, shrub exposure enhanced melt energy due to greater longwave and sensible heat fluxes than snow. Moreover, the presence of an organic surface layer on northern mineral soils, with very high hydraulic conductivity values when compared with the underlying mineral soil, plays a critical role in controlling the rate of subsurface drainage from slopes when frozen grounds begin to thaw (Quinton *et al.*, 2005). This differs from sparsely vegetated alpine environments with impermeable substrates and poor soil development, where it has been reported that the runoff dynamics depend primarily upon an accurate description of the energy balance and less on the distribution of vegetation and soil characteristics (Lehning *et al.*, 2006).

Incorporating basin heterogeneity to better describe and predict hydrological processes within numerical models has led to a number of methods of basin segmentation. However, given the heterogeneity in the landscape, hydrologists are forced to conceptualise the physics to some degree and seek effective parameter values (Pietroniro & Soulis, 2003). This is especially important in remote regions such as northern Canada, where soils, vegetation and topography are not well inventoried. Distributed hydrological models use aggregation methods to account for landscape variability and process representation; and a critical point in the application of these models is the selection of a landscape element size. The choice of model resolution determines what kinds of variability can be explicitly and implicitly represented (Grayson & Blöschl, 2001). Most snow energetics, snow hydrology and snow-atmosphere interaction models still do not account for slope and aspect, solar angle and sky-view effects, and their respective scales of influence (Pomeroy *et al.*, 2003). However, those that include these effects show substantial impact on the timing, area and duration of snowmelt (e.g. Marks *et al.*, 2002). Recent research on hydrological processes in northern mountains has led to an improved process understanding (e.g. Quinton & Gray, 2001; Pomeroy *et al.*, 2004; Essery & Pomeroy, 2004; Sicart *et al.*, 2004; Quinton *et al.*, 2005; Carey & Quinton, 2005; McCartney *et al.*, 2006); however, few studies have examined the spatial and temporal variability of these processes and their applicability for runoff prediction at different scales.

The objectives of this paper are two-fold: (a) to investigate the effects of different physically-based spatial model aggregations and parameterisations in describing the main hydrological processes affecting snow-cover ablation and basin runoff during spring snowmelt; and (b) to assess the suitability of a simple and conceptual soil moisture balance and flow routine for runoff generation during snowmelt in a permafrost environment.

The philosophical basis of the modelling approach is the desire to describe the processes in as physically-realistic a manner as possible, given the availability of data and parameters to run the model. Hence, snowmelt and infiltration into frozen soils are described using physically-based algorithms with *a priori* parameter sets (deductive approach), whilst changes in runoff generation mechanisms as a consequence of the ability of the organic layer and soil profile to hold water as the thaw progresses, are conceptually formulated. On the other hand, a downward or inductive (Sivapalan *et al.*, 2003b) modelling approach is used for basin segmentation based

on the understanding of the controls of the hydrological responses such as topography, vegetation and soils.

## STUDY AREA

The study was conducted in Granger Basin ( $60^{\circ}31'N$ ,  $135^{\circ}07'W$ ), which is located within Wolf Creek Research Basin, 15 km south of Whitehorse, Yukon Territory, Canada (Fig. 1). The mean annual temperature is approximately  $-3^{\circ}C$ , with monthly mean temperatures ranging from  $5$  to  $15^{\circ}C$  in July and from  $-10$  to  $-20^{\circ}C$  in January. The mean annual precipitation varies between 300 and 400 mm, with approximately 40% falling as snow (Pomeroy & Granger, 1999). The geological composition of Granger Basin is primarily sedimentary, consisting of sandstone, siltstone, limestone and conglomerate, overlain by glacial till ranging in thickness from a few centimetres to 10 m. The presence of permafrost is determined by temperature and aspect, thus it is found under the NF slopes and in higher elevations, whereas seasonal frost occurs on the SF slopes. All soils are fully frozen at the time of snowmelt. In lower elevation regions of Granger Basin, soils are capped by an organic layer up to 0.4 m thick, consisting of peat, lichens, mosses, sedges and grasses (Carey & Quinton, 2005).

The study catchment comprises an area of  $8\text{ km}^2$  and ranges in elevation from 1310 to 2100 m a.m.s.l. The landscape shows a gradient from a shrub-tundra environment at lower elevations to an alpine environment at higher elevations. Five main distinct landscapes were identified according to both field observations of vegetation cover, soils and permafrost, slope and exposure, and the basin units described by McCartney (2006). Differences in the number of these landscape units reflect the aggregation performed for modelling reasons (i.e. reduce the degrees of freedom) over very similar areas with no distinguishable snowmelt rates. Therefore, the basin segmentation was focused on the main processes that govern snowmelt, such as wind exposure controlling the pre-melt snow accumulation and slope controlling the snowmelt energetics.

Table 1 summarises the characteristics of the identified landscapes. The upper basin (UB), located between 1600 and 2100 m a.m.s.l. in the lee side of Mount Granger, has a northeast oriented  $15^{\circ}$  slope. Colder climate conditions and exposure result in a very sparse vegetation cover where grasses, lichens and mosses prevail. No organic layer is observed and the mineral soil is generally exposed. A small perennial snowpack in the upper reaches of the UB is evidence of the climate and snow drift inputs from upwind catchments. The plateau (PLT) area expands over an

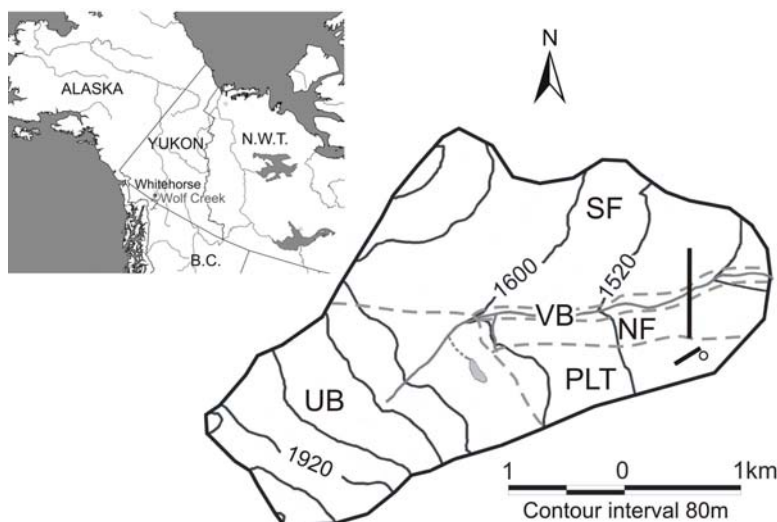


**Fig. 1** Granger Basin within Wolf Creek Research Basin. Circle and lines indicate the locations of the met station and measurement transects, respectively.

**Table 1** Physiographic characteristics of the landscapes units at Granger Basin. Vegetation cover and soil type were adapted from McCartney (2006).

Landscape	Area (km <sup>2</sup> )	Elevation range (m)	Vegetation cover	Soil type
Upper basin (UP)	2.5	1600–2100	Bare ground	Mineral/rocks
Plateau area (PTL)	1	1460–1520	Short shrubs (<0.3 m)	Mineral + thin organic layer (<0.1 m)
North-facing slope (NF)	1	1350–1460	Mixed shrubs (0.3–1 m)	Thick organic layer (0.25 m) + mineral
South-facing slope (SF)	3	1350–1760	Mixed shrubs (0.3–1 m)	Organic layer (0.12 m) + mineral
Valley bottom (VB)	0.5	1310–1350	Tall shrubs (>1 m)	Organic layer (0.14 m) + mineral

area of 1 km<sup>2</sup> at an elevation of 1500 m a.m.s.l. and its vegetation cover is characterised by short shrubs (<0.3 m). Mineral soil prevails with a thin organic layer. The NF slope is where the organic layer is more significant and continuous permafrost is observed. It is located near the basin outlet and comprises an area of approximately 1 km<sup>2</sup>. Vegetation cover is composed by a mix of tall (1 m) and short (0.3 m) shrubs. The SF slope, with similar vegetation cover to the NF slope, expands on the north fringe of the basin covering an area of approximately 3 km<sup>2</sup>. The organic layer is less significant, whereas a discontinuous permafrost with a patchy structure is observed at the beginning of the melt season. The valley bottom (VB) includes the lower reach of Granger Creek near the basin outlet. It is characterized by a significant presence of organic layer and by tall shrubs (1–2 m).

## SNOWMELT RUNOFF MODELLING

### Modelling approach

The effects of different aggregation methods on modelling snowmelt ablation and runoff generation in a mountainous arctic environment were evaluated by comparing aggregated and distributed tiles (Fig. 2). The model aggregation is based on the hydrological response unit (HRU) concept, introduced by Flügel (1995), which can be understood as an areal entity characterised by certain similar hydrological and geomorphological properties. The selection of the modelling units was based on the understanding of the main processes that govern snowmelt (i.e. snow accumulation, snow redistribution, and snow energetics) in sub-tundra mountainous environments. As a result, five main landscape units (i.e. UB, PLT area, NF and SF slopes, and VB), which are presumed to approximate HRUs, were identified and used for basin segmentation according to their vegetation cover, soils and permafrost, slope and exposure (see Table 1). For example, north-facing slopes and shrub-tundra areas act as accumulation zones, while spring melt rates are much higher on south-facing slopes due to increased incident solar radiation. Clearly, it is an arbitrary criterion; however, given the difficulty, or impossibility, of finding an optimum element size that can compromise measurements, processes and modelling scales (Blöschl, 1999), the present approach for basin segmentation (i.e. inductive) balances data availability with the desired resolution of the predictions (i.e. identification of differential snowmelt rates between landscape units).

In the aggregated model, all the landscape units were aggregated in a single, flat HRU. In this case, initial conditions (mean SWE, mean soil moisture) and forcing data (mean radiation and mean air temperature) were weight-averaged according to the area of the landscape unit (see Fig. 2(a)). For the distributed or especially aggregated analysis, the basin was divided into different HRUs according to the landscape units (see Fig. 2(b)). Exposure and, subsequently, vegetation and soil types, were the main criteria used to define landscape units.

Furthermore, this comparison allowed for the estimation of uncertainties in input data, whereas uncertainties in both model structure and model parameters were evaluated using the

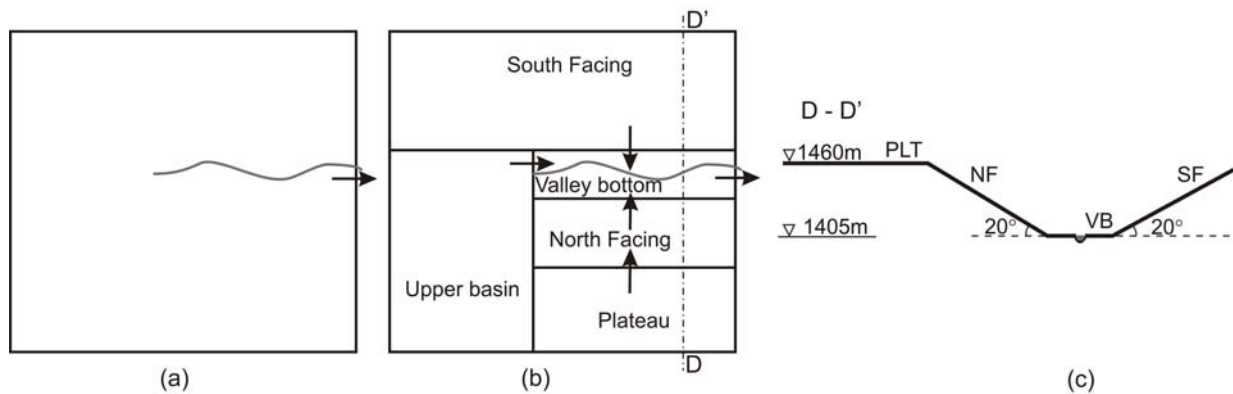


**Fig. 2** Schematic representation of the basin: (a) aggregation of the different landscapes in one single and flat HRU; (b) distribution of the HRUs according to landscape units; and (c) profile exhibiting differences in elevation and exposure among HRUs. Arrows indicate flow direction.

combined physically-based and conceptual modelling approach. Thus, uncertainties in the representation of hydrological processes that can be described physically (e.g. snow-cover ablation, infiltration into frozen soils) are reduced by using a deductive modelling approach, while the inductive approach, or a conceptual representation, is adopted for those processes less well understood in this environment (e.g. spring soil water storage dynamics, snowmelt runoff generation).

**Model description**

The version of the Cold Regions Hydrological Model (CRHM) used for this analysis included several modules which have been applied to the generic framework described by Pomeroy *et al.* (2007). Figure 3 depicts the relevant modules and the forcing data used in this application. Two main subdivisions can be identified: (1) physically-based modules, which include algorithms developed using the physical principles governing processes, such as energy balance snowmelt, evaporation and infiltration into frozen soils; and (2) conceptual modules, which represent processes that are less well understood, such as the soil moisture balance and flow routing.

Forcing of the data is handled in the OBSERVATION module. The main features of this module include the use of a threshold temperature parameter (0°C) to distinguish between snow-fall and rainfall events, and a lapse-rate correction (6.5°C/1000 m) to account for elevation effects.

The GLOBAL module accomplishes the partitioning of the incoming solar radiation according to slope and aspect, and cloudiness effects. Direct shortwave radiation ( $K_{dir}$ ), diffuse shortwave radiation ( $K_{dif}$ ), and a cloudiness index ( $c$ ) are calculated using expressions proposed by Garnier & Ohmura (1970). The cloudiness index ( $c$ ) is determined from the comparison between the observed incoming shortwave radiation ( $K$ ) and the theoretical clear sky direct-beam component of solar radiation ( $K_{theo}$ ) over flat areas, and is then used to calculate  $K_{dir}$  on slopes having some aspect. The contribution of diffusive sky radiation,  $K_{dif}$ , is first estimated for flat areas (List, 1968) using the extra-terrestrial solar irradiation on a horizontal surface at the outer limit of the atmosphere  $K_{ext}$ , and then corrected by slope and aspect following Garnier & Ohmura (1970). Net radiation and ground heat flux are calculated in the NETALL module using the algorithm presented by Satterlund (1979) for estimating daily net longwave radiation and presuming that ground heat flux is proportional to net radiation. Net radiation calculated in the NETALL module is not used for snowmelt calculations, but for evapotranspiration.

Snow-cover albedo is estimated in the ALBEDO module, which assumes that the albedo depletion of a shallow snow cover, not subject to frequent snowfall events, can be approximated by three line segments of different slope describing the periods: pre-melt, melt and post-melt (the period immediately following disappearance of the snow cover). This approach was based on

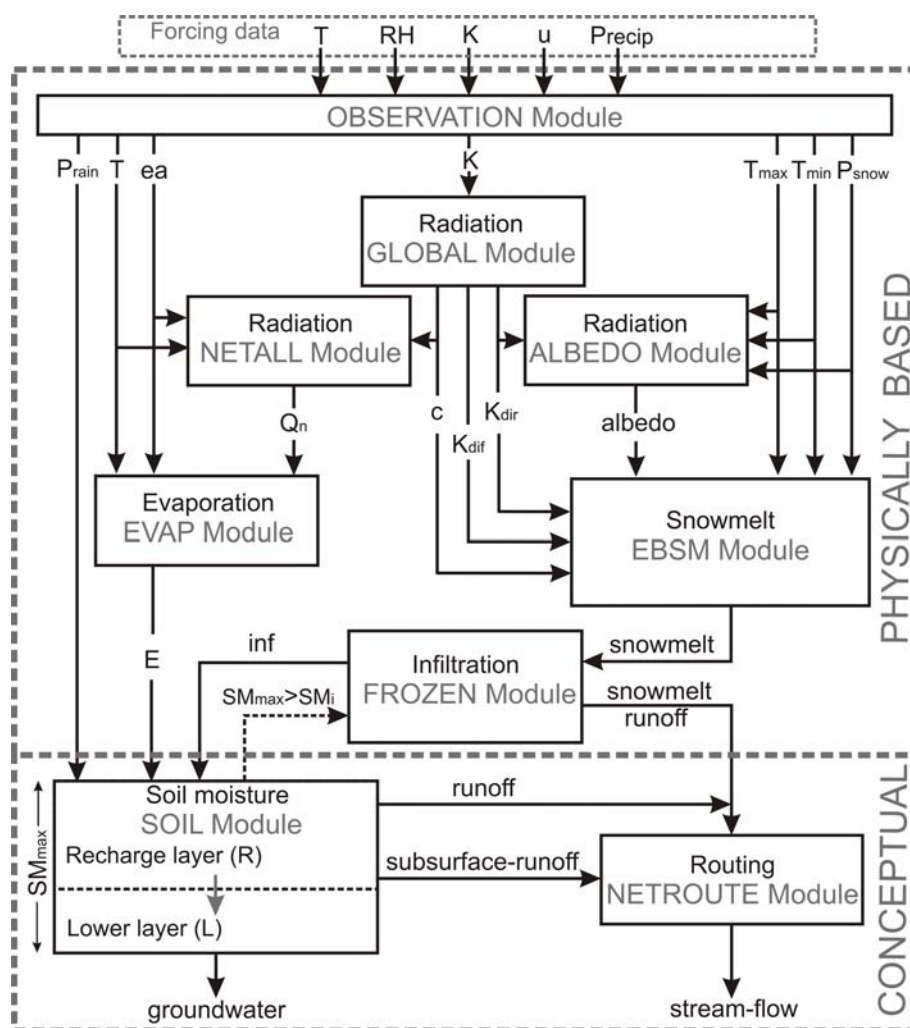


**Fig. 3** Outline of the modular structure of the CRHM model used. Solid arrows indicate module input/outputs. Dashed arrow indicates module feedback.  $T$ : air temperature ( $^{\circ}\text{C}$ ),  $\text{RH}$ : relative humidity (%),  $K$ : incoming shortwave radiation ( $\text{W}\cdot\text{m}^{-2}$ ),  $u$ : wind speed ( $\text{m s}^{-1}$ ),  $\text{Precip}$ : precipitation (mm),  $e_a$ : water vapour pressure (Pa),  $T_{\text{max}}$ : daily maximum air temperature ( $^{\circ}\text{C}$ ),  $T_{\text{min}}$ : daily minimum air temperature ( $^{\circ}\text{C}$ ),  $K_{\text{dir}}$ : direct shortwave radiation ( $\text{W}\cdot\text{m}^{-2}$ ),  $K_{\text{dif}}$ : diffuse shortwave radiation ( $\text{W}\cdot\text{m}^{-2}$ ),  $c$ : cloudiness index,  $Q_N$ : net radiation ( $\text{W}\cdot\text{m}^{-2}$ ),  $P_{\text{snow}}$ : snowfall (mm),  $P_{\text{rain}}$ : rainfall (mm),  $E$ : evapotranspiration (mm),  $\text{SM}_{\text{max}}$ : maximum soil moisture content (mm),  $\text{SM}_i$ : actual soil moisture content (mm),  $\text{inf}$ : infiltration.

several years of point and areal measurements of reflected shortwave radiation during the snowmelt period (Gray & Landine, 1987).

Snow-cover ablation is estimated using the Energy-Budget Snowmelt Model (EBSM module) (Gray & Landine, 1988). The model uses the snowmelt energy equation (equation (1)) as its physical framework, and physically-based procedures for evaluating radiative, convective, advective, and internal-energy terms from standard climatological measurements:

$$Q_M + Q_N + Q_H + Q_E + Q_G + Q_D = \frac{dU}{dt} \quad (1)$$

where  $Q_M$  is the energy available for snowmelt,  $Q_N$  is the net radiation,  $Q_H$  is the turbulent flux of sensible heat,  $Q_E$  is the turbulent flux of latent energy,  $Q_G$  is the ground heat flux,  $Q_D$  is the advection energy from external sources, and  $dU/dt$  is the flux rate of change of internal energy in the snowpack. All units are in  $\text{W m}^{-2}$ .

Daily estimates of net radiation, maximum and minimum air temperature, a threshold air temperature for melt initiation, and snow-cover and snowfall depths to establish the “start” of the melt and albedo depletion rate are used to drive the EBSM. The net radiation is calculated for the pre-melt period as follows:

$$Q_N = -0.04 + 0.76 \underbrace{\left[ Q_0 \left[ 0.052 + 0.052 \frac{n}{N} \right] (1 - A) + 0.097 \sigma T_a^4 \right]}_{\text{net shortwave term}} \underbrace{\left[ (-0.39 + 0.093 e_a^{0.5}) \left( 0.26 + 0.81 \frac{n}{N} \right) \right]}_{\text{net longwave term}} \quad (2)$$

and for the melt period:

$$Q_N = -0.53 + 0.47 Q_0 \left[ 0.52 + 0.52 \frac{n}{N} \right] (1 - A) \quad (3)$$

where  $Q_0$  is the daily clear-sky shortwave radiation incident to the surface ( $\text{MJ m}^{-2} \text{d}^{-1}$ ),  $n$  is the number of hours of bright sunshine in the day,  $N$  is the maximum possible number of hours of bright sunshine in the day,  $A$  is the mean surface albedo,  $\sigma$  is the Stefan-Boltzmann constant ( $4.9 \times 10^{-9} \text{ MJ m}^{-2} \text{K}^{-4} \text{d}^{-1}$ ),  $T_a$  is the mean daily air temperature (K), and  $e_a$  is the mean daily vapour pressure of the air (mbar). The ratio  $n/N$  can be estimated from  $c$ , the cloudiness index, using shortwave radiation measurements if sunshine hours are unavailable (as in this application).

Turbulent transfer of sensible and latent heat is derived from boundary layer flux–profile relationships, whereas the amount of melt,  $M$ , is calculated from  $Q_m$  (equation (4)). Daily melt ( $\text{mm d}^{-1}$ ) can be approximated by  $M = 0.270 Q_m$  when  $Q_m$  is in  $\text{W m}^{-2}$ . The fluxes directed towards the snowpack are taken as positive whereas those directed away are negative:

$$M = \frac{Q_m}{\rho_w B h_f} \quad (4)$$

where  $\rho_w$  is the density of water ( $1000 \text{ kg m}^{-3}$ ),  $B$  is the thermal quality of the snow or fraction of ice in a unit mass of wet snow ( $B$  usually ranges from 0.95 to 0.97) and  $h_f$  is the latent heat of fusion of ice ( $3.335 \times 10^5 \text{ J kg}^{-1}$ ).

The change in internal energy ( $dU/dt$ ) of the snowpack is estimated using an algorithm that assumes a minimum state of internal energy determined by the minimum daily temperature, a maximum state equal to zero, a maximum liquid-water-holding content of the snow cover equal to 5% by weight, a snow-cover density of  $250 \text{ kg m}^{-3}$ , and no melt unless indicated by the model.

During the spring snowmelt, infiltration into frozen soils is estimated in the FROZEN module using the approach proposed by Zhao & Gray (1999) and Gray *et al.* (2001). This module divides the soil into restricted, limited and unlimited classes according to its infiltration characteristics. When limited, infiltration is governed primarily by the snow-cover water equivalent (SWE) and the frozen water content of the top 40 cm of soil. The frozen infiltration routine is disabled when the SWE of the snowpack is less than 5 mm. The cumulative snowmelt infiltration (mm) into frozen soils is computed as:

$$\text{INF} = C S_0^{2.92} (1 - S_I)^{1.64} \left( \frac{273.15 - T_I}{273.15} \right)^{-0.45} t_0^{0.44} \quad (5)$$

where  $C$  is a coefficient,  $S_0$  is the surface saturation ( $\text{mm}^3 \text{mm}^{-3}$ ),  $S_I$  is the average soil saturation (water + ice) of 0–40 cm soil at the start of infiltration ( $\text{mm}^3 \text{mm}^{-3}$ ),  $T_I$  is the average temperature of the 0–40 soil layer at the start of infiltration (K), and  $t_0$  is the infiltration opportunity time (h).

Infiltration opportunity time is estimated as the time required to melt a snow cover assuming continuous melting and small storages and evaporation. Thus,  $t_0$  is calculated by cumulating the hours when there is snowmelt according to the EBSM module.

Actual evapotranspiration is estimated in the EVAP module using the algorithm proposed by Granger & Gray (1989) and Granger & Pomeroy (1997). This algorithm is an extension of the Penman equation for unsaturated conditions. The ability to supply water for evaporation is indexed

using only the atmosphere aridity, so no knowledge of soil moisture status is required for this module. To ensure continuity, however, evaporation is taken first from any intercepted rainfall store, then from the upper soil layer and then from the lower soil layer, and restricted by water supply in the following module (see Pomeroy *et al.*, 2007).

Variations in the soil moisture balance are conceptually represented as a two-layer soil profile in the SOIL module. The upper layer or recharge layer, represents the topsoil and is where infiltration and evaporation occur. Transpiration is withdrawn from the entire soil profile. Snowmelt infiltration computed using the FROZEN module occurs when soil moisture capacity is available in the soil profile, otherwise *snowmelt runoff* is generated. Excess water from both soil layers constitutes runoff. Runoff is generated when rainfall events exceed the soil moisture capacity and when the groundwater recharge has been satisfied. Snowmelt runoff and runoff are added together in the term that represents the *overland flow*. Furthermore, a horizontal soil leakage, *subsurface runoff*, continuously diminishes the amount of water in the soil and follows an exponential or linear reservoir decay:

$$K_{\text{ssr}} = \frac{R_i}{R_{\text{max}}} \quad (6)$$

where  $K_{\text{ssr}}$  is horizontal soil leakage ( $\text{T}^{-1}$ ), and  $R_i$  (mm) and  $R_{\text{max}}$  (mm) are the actual and maximum soil moisture capacity in the recharge or top layer, respectively.

Outflow from an HRU, constituted by runoff and subsurface runoff flows, and eventually inflow from another HRU, are independently routed in the NETROUTE module using a hydraulic routing approach. Each flow is calculated by lagging its inflow by the travel time through the HRU, then routing it through an amount of linear storage defined by the storage constant,  $K$ . For a given HRU, the upstream inflow is conceptualised as the outflow from the upstream HRU, whereas runoff accounts for overland flow, and soil storage effects are considered in the subsurface runoff component.

### Observations and forcing data

Meteorological measurements of air temperature, relative humidity, incoming solar radiation, and both wind speed and direction for two snowmelt periods from 17 April to 10 June 2002 and from 17 April to 31 May 2003, were used to force the modules within CRHM. Observations were made on the PLT area, with the exception of precipitation data obtained from a nearby station located approximately 1 km from the study site within Wolf Creek Research Basin. The precipitation data were not corrected due to the insignificant amounts (<5 mm) recorded during the study periods in both years.

Areal snow water equivalent (SWE) was calculated from snow survey observations for each of the landscape units, such as PLT area, NF and SF slopes, and VB, in 2002 and 2003, respectively. Snow surveys consisted of transects where both snow depth and density were measured every 5 and 10 m, respectively. Length of the transects varied as a function of the landscape heterogeneity; thus, when the snow cover was continuous, approx. 25 points were measured in the PLT area, whereas 20 were measured in the NF and SF slopes, and six points in the VB (for more details see McCartney *et al.*, 2006). Observations of the dynamics of the SWE reflect the differences in terms of snow accumulation and ablation between the landscape units.

The aggregated model was initialised by computing the spatially-weighted average values from each landscape. Therefore, basin average values of elevation, SWE, albedo and soil moisture were estimated. The distributed model was initialised using calculated SWE values from available snow surveys at the different HRUs. Average SWE values from the PLT area and NF slope in 2002 were assigned to the UB, assuming that the UB comprises characteristics of the NF slope and the PLT area because of its northeast orientation. Since no substantial differences in the snow cover were seen prior to the snowmelt, all HRUs were initialised with the same albedo value of 0.83, determined using radiometric measurements in Granger Basin (Bewley *et al.*, 2007). Liquid



water content measured in the previous autumn prior to freeze-back (Carey & Quinton, 2005; Quinton *et al.*, 2005) was used as the pre-melt soil moisture content. Streamflow data were measured on Granger Creek, close to the basin outlet.

**Model calibration**

Model calibration was performed on the conceptual modules, whereas the parameter values of the physically-based modules were derived experimentally. Therefore, calibration was only performed on discharge data by tuning the parameters of both the SOIL and NETROUTE modules to fit the observed hydrograph.

A melt delay parameter was set up in the EBSM module to adjust for the start of the melt, since no winter model runs were performed to compute the internal energy of the snow pack prior to melt. Parameter values describing infiltration into frozen soils were set in consideration of the results of field studies (e.g. Zhao & Gray, 1999; McCartney *et al.*, 2006). Thus, given their conceptual description,  $C = 2$  and  $S_0 = 1$ , were assumed to have the same value for all HRUs. Table 2 shows the  $S_i$  and the calculated  $t_0$  values for each HRU.

Water storage potential for each HRU comprises water stored in both the organic and mineral soils, and in depressional storage. Field observations demonstrate that surface depression storage is very important towards the end of the melt season in the PLT area, NF slope and VB. While the limits of depressional storage values are uncertain, a 300 mm water storage potential was defined for each HRU, regardless of the presence of an organic layer, permafrost, or the dissimilar proportion of unfrozen and frozen soil moisture. This value was estimated considering previous calculations, which included an estimation for the NF slope of about 230 mm of total moisture (water + ice) in the upper 40 cm of soil (Quinton *et al.*, 2005), while initial basin storage of 180 mm was estimated for the same depth in the NF and SF slopes, based upon soil moisture profiles at three soil moisture probes (TDR) by Carey & Quinton (2004). Soil parameter calibration was undertaken manually and was based on previous basin knowledge (see Table 2). Since percolation to groundwater in the SOIL module is only active when there is soil water excess, subsurface runoff values ( $K_{ssr}$ ) were lagged in the NETROUTE module to account for groundwater losses due to macropore flow and through other mechanisms not properly represented in the SOIL module. As a result, the PLT area and NF slope had the HRUs with the largest amounts of lagged subsurface runoff, followed by the SF slope. Both the *Lag* parameter and an additional *K* storage parameter were adjusted for each flow in the NETROUTE module to account for different travel times between HRUs (see Fig. 3). Due to the late and continuous snowmelt season of 2002, *K* storage values were assigned only to the NF slope. However, for 2003, with discontinuous snowmelt events, large *K* storage values for the UB and the PLT area were needed to account for differences in timing.

**Table 2** Model parameter values for each landscape unit for the FROZEN, SOIL and NETROUTE modules.

Parameter	UB	PLT	NF	SF	VB
$S_i$ ( $\text{mm}^{-3} \text{mm}^{-3}$ )	0.25	0.20	0.34	0.25	0.25
$t_0$ for 2002 (h)	504	408	432	408	480
$t_0$ for 2003 (h)	360	312	528	504	360
Initial soil moisture for 2002 (mm)	270	200	300	190	260
Initial soil moisture for 2003 (mm)	200	200	200	260	300
$K_{ssr}$ for 2002 ( $\text{d}^{-1}$ )	0	20	4	1	1
$K_{ssr}$ for 2003 ( $\text{d}^{-1}$ )	0	0.50	0	0.50	0
<i>K</i> storage for 2002 (d)	0	0	1	0	0
<i>K</i> storage for 2003 (d)	12	4	0	1	0

$S_i$ : average soil saturation (water + ice) of 0–40 cm soil at the start of infiltration;  $t_0$ : calculated infiltration opportunity time;  $K_{ssr}$ : horizontal soil leakage; *K*: linear storage constant.

## RESULTS AND DISCUSSION

### Ablation

Figure 4 illustrates the comparison of the simulated snowpack ablation using the aggregated and distributed modelling approaches with their respective observed values. Observations represent the spatially-weighted average of those landscape units where snow survey data were available. Thus, only the NF and SF slopes and VB were considered. In order to compare both modelling approaches, outputs from the distributed model for the considered HRUs were re-aggregated using a spatially-weighted average. In order to compare the model performances of the aggregated and distributed approaches, two efficiency criteria for evaluating snow-cover ablation were computed: the average melt rate (AMR) by dividing the initial SWE at the start of the simulation period by the number of days till the average snow cover in each HRU disappeared; and the standardised root mean square error (SRMSE), normalized with respect to the mean of the observed values (Table 3). For the 2002 snowmelt season, modelled and observed snow ablation rates were similar at the early stages of the snowmelt season for both the aggregated and the distributed models, respectively. However, more substantial differences between modelled and observed values were seen during the late stages. The aggregated model showed more rapid depletion than the re-aggregated distributed model or the observed data. In contrast, the aggregated model dramatically failed to predict the observed snow ablation rates for 2003, while the distributed results showed a very similar performance to that for 2002, with some differences at the late stages of the snowmelt

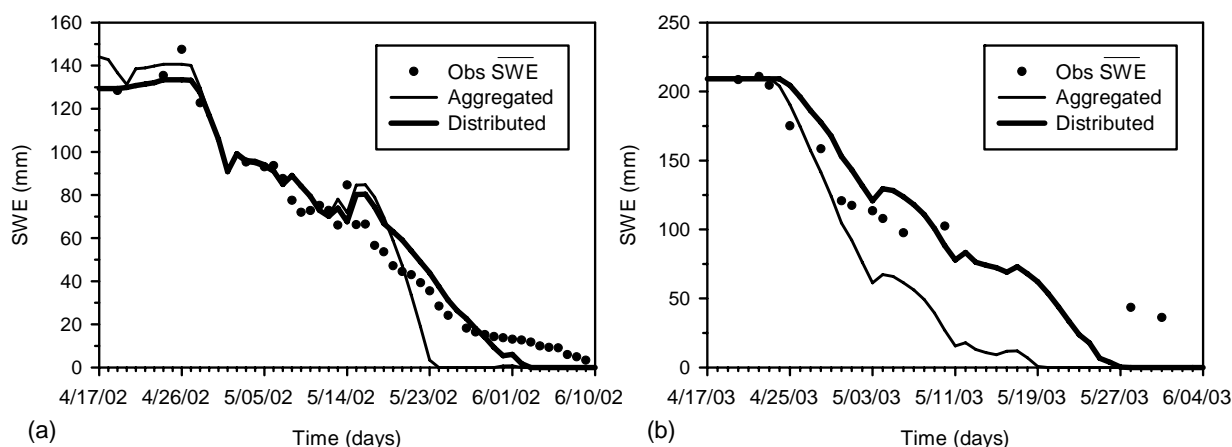


**Fig. 4** Comparison between observed and the simulated SWE values using the aggregated and distributed models. Values represent the spatially-weighted basin-averages using NF and SF slopes, and VB observations. (a) 2002 and (b) 2003.

**Table 3** Comparison of model performances in describing snow-cover ablation and basin runoff.

Year	SWE <sub>AGR</sub>	SWE <sub>DIST</sub>	AMR (mm/d)				SWE <sub>PLT</sub>	Q <sub>AGR</sub>	Q <sub>DIST</sub>
			SWE <sub>NF</sub>	SWE <sub>SF</sub>	SWE <sub>VB</sub>	$r^2$			
2002	3.79 (+62)	3.42 (+46)	4.58 (+20)	2.66 (+6)	4.36 (-15)	-	0.35 (+10)	0.37 (+7)	
2003	6.18 (+60)	5.00 (+29)	6.62 (+19)	4.07 (+17)	5.80 (+41)	7.17 (+12)	0.19 (+100)	0.60 (+37)	
SRMSE								SRMSE	
2002	0.26	0.27	0.15	0.27	0.79	-	0.73	0.48	
2003	0.18	0.18	0.62	0.20	0.29	0.12	1.79	0.83	

AMR: average melt rate along the simulation period, SRMSE: standardised RMSE by the mean value,  $r^2$ : coefficient of determination.

AGR: aggregated simulation; DIST: distributed simulation.

The % differences between modelled and observed average snowmelt rates are shown in parentheses. Square brackets indicate the % difference between modelled and observed runoff volume.

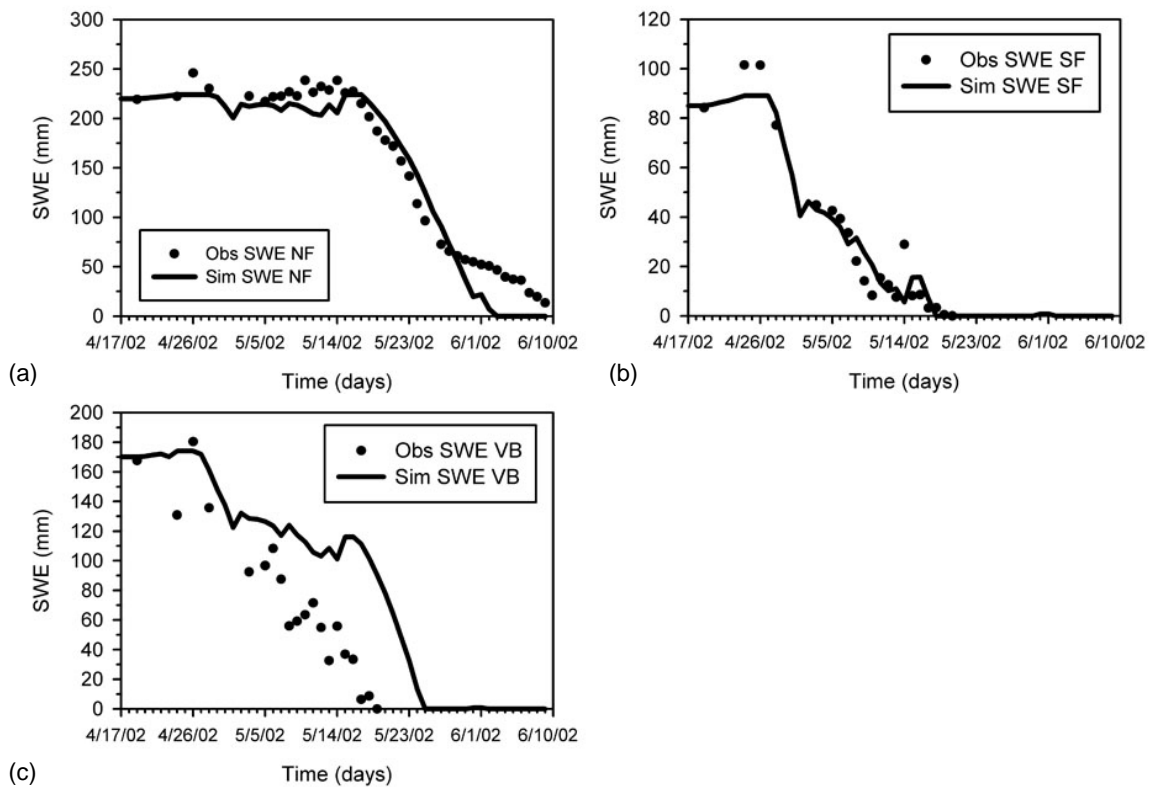


**Fig. 5** Distributed observed and simulated areal SWE values at different landscapes for 2002: (a) NF slope, (b) SF slope, and (c) VB.

season. However, each model had similar performances for both years, the distributed model being the one with the closest estimates. The distributed model showed the lowest differences in observed AMR, with SRMSE values of 0.18, whereas the aggregated model showed larger differences of the snowmelt rates and SRMSE values of 0.26 and 0.27 for 2002 and 2003, respectively.

Distributed SWE simulations during the ablation of the snow cover are shown in Figs 5 and 6 for 2002 and 2003, respectively. In general, they illustrate a very good representation of both the evolution and the differential melt rates observed for each of the landscape units considered, although differences in the observations are usually seen towards the end of the melt season. Simulated SWE values at the NF slope (Figs 5(a) and 6(a)) showed close agreement with observed values during the main melt event in the middle of the melt season; however, the differences observed at the beginning and end of the 2003 melt season reduced the model efficiency from SRMSE values of 0.15 in 2002 to 0.62 in 2003. This is attributed to episodic inputs of blowing snow in this HRU throughout the melt period, with substantial accumulation becoming apparent by the end of melt phenomena that could not be represented at the scale used. This HRU is fed by blowing snow, even when other HRUs are ablating (Pomeroy *et al.*, 2003). Simulated values for the SF slope showed an accurate description of the observed evolution of the snow-cover ablation for the entire melt season for 2002 (Fig. 5(b)) with a SRMSE value of 0.27. In 2003, even when differences in the late stage simulations were seen (Fig. 6(b)), due to the persistence of a snow drift that melted approximately 10 days later than predicted by the model, a similar model performance with a SRMSE of 0.20 was observed. In the VB, simulation results for the studied years were dissimilar; a good description (SRMSE = 0.29) of the observed SWE values was modelled in 2003 (Fig. 6(c)), whereas in 2002, modelled melt rates on average were lower than the observed values throughout the melt period, particularly at later stages (Fig. 5(c)), which reduced the model efficiency to a SRMSE of 0.79. This is attributed to the progressive exposure of tall shrubs (2–3 m)

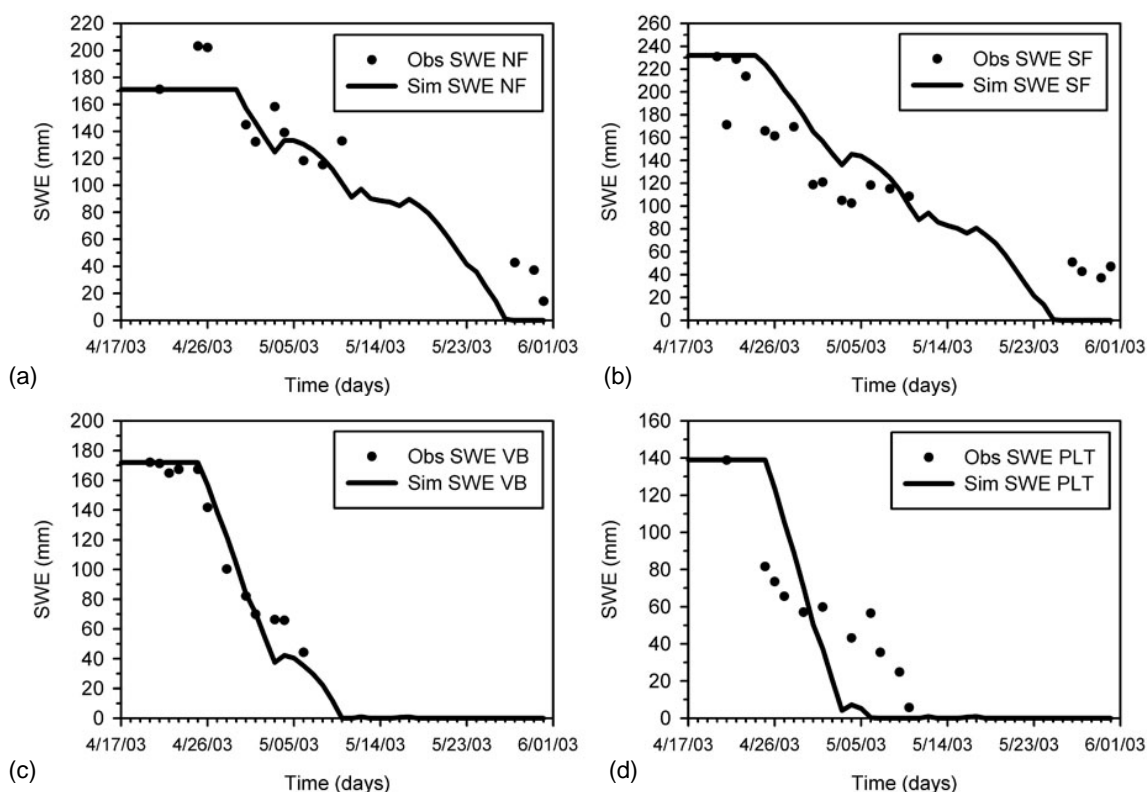


**Fig. 6** Distributed observed and simulated areal SWE values at different landscapes for 2003: (a) NF slope, (b) SF slope, (c) VB, and (d) PLT area.

that enhance longwave radiation and sensible heat to the snowpack and hence the increase of melt rate (Pomeroy *et al.*, 2006). This canopy effect is not considered in this model, but will be in subsequent developments according to the findings of Bewley *et al.* (2007). Simulated snowmelt rates in the PLT area (Fig. 6(d)) were faster than those observed in 2003, with larger differences at both the early and late stages of the snowmelt season. This lack of agreement resulted from the inclusion of the last two points of the snow survey transect with tall shrubs that affected the overall areal SWE calculation, as a consequence of large snow accumulation amounts and drastic changes in albedo due to sudden branch emerging.

In general, the simulated AMRs were overestimated in all the landscape units (see Table 3). Descriptions of SWE depletion on the SF slope were the ones that best agreed with those computed from the observed values. Similar behaviour was observed when the SRMSE values of each landscape unit were compared. Conversely, the VB was the landscape unit with the worst descriptions of snow-cover ablation, possibly due to the importance of local-scale advection of energy to melting snow from both tall shrubs and bare ground at this site (Granger *et al.*, 2006).

### Snowmelt runoff

Snowmelt runoff response proved to be very sensitive to differential snowmelt rates (Fig. 7). An uninterrupted snowmelt event resulting in a single peak hydrograph was observed for 2002, whereas a multi-peak hydrograph showed the effect of discontinuous melt due to a sequence of warmer and colder periods in 2003 (McCartney *et al.*, 2006; Quinton *et al.*, 2005). Moreover, since snowmelt discharge volumes represent only 50 and 35% of the winter snowpack for 2002 and 2003, respectively, and baseflow before melt is relatively constant ( $\sim 7 \text{ L s}^{-1}$ ), it is suggested that either the snowmelt does not all immediately contribute to spring runoff due to soil water storage effects, or it shows up downstream. For example, Carey & Woo (2000) found that snowmelt runoff represents 80% of the winter snowpack in Wolf Creek Research Basin for a NF slope with

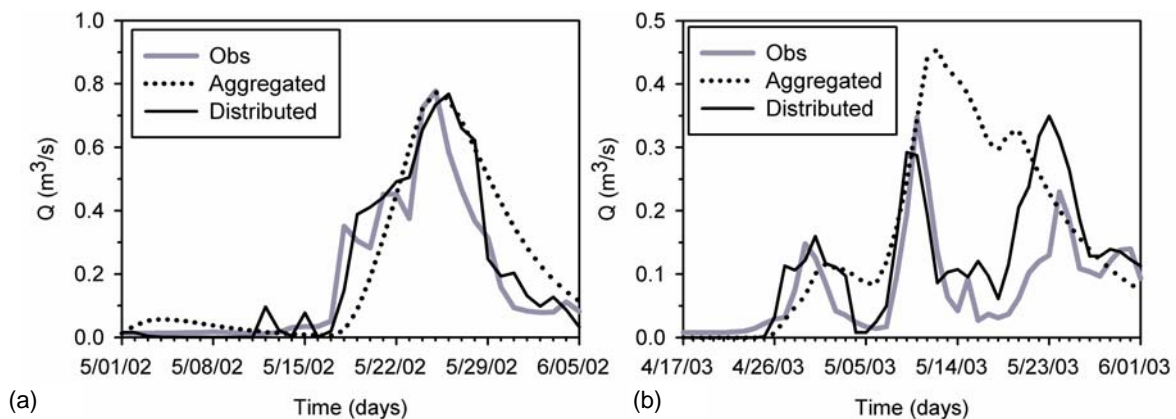


**Fig. 7** Observed vs simulated basin discharge: (a) 2002 and (b) 2003.

an open forest (black and white spruce) and continuous permafrost. The organic layer transmitted 21% of the runoff while 53 and 26% came from rill and matrix flows, respectively. This runoff deficit made it difficult to properly close the basin water balance during the spring snowmelt season.

Figure 7(a) illustrates that, for 2002, both modelling approaches had good overall performance in terms of runoff volumes and peak runoff, with SRMSE values of 0.73 and 0.48 for the aggregated and distributed approaches, respectively. The aggregated model showed differences in the timing of the rising and falling limbs of the hydrograph, whereas the distributed model accurately described the hydrograph shape. Similar results were found by Dornes *et al.* (2006) using a simplified version of the infiltration into frozen soil and soil moisture modules, which suggest that parsimonious models can provide an accurate description of single and continuous snowmelt events. However, a dissimilar performance amongst the models was observed for 2003 (Fig. 7(b)). Although some differences were seen, the distributed model was able to reproduce the timing of the three observed snowmelt peaks, though overpredicting the magnitude of the last peak. Conversely, the aggregated model was unable to replicate multiple peaks in the observed hydrograph because the influences of the differential snowmelt rates among landscape units on response and timing of snowmelt runoff are not explicitly represented. These findings were assessed objectively by the use of two efficiency criteria (see Table 3): the coefficient of determination ( $r^2$ ) defined as the squared value of the coefficient of correlation, and the SRMSE. The relatively low efficiency criteria values reflect that the model was not optimized, but allowed to retain physically-based parameters; differences in the values reflect the improved performance of the distributed over the aggregated model approach. Thus, the aggregated model showed SRMSE values of 0.73 and 1.79 for the 2002 and 2003 snowmelt seasons, respectively, whereas the distributed model had values of 0.48 and 0.83 for the same periods.

## CONCLUSIONS

The effects of different aggregation methodologies in modelling snow-cover ablation and basin runoff for a small basin in a high latitude, mountainous environment were evaluated. From the comparison of the two model aggregation approaches, the distributed approach best described the observed magnitudes of both snow-cover ablation and basin runoff. Conversely, the aggregated approach could not properly represent the evolution of the differential snowmelt rates during the course of the snowmelt period. Late stages of melt modelled by the aggregated approach showed substantial differences with faster snowmelt rates compared with observations. Basin runoff predictions showed a dissimilar performance between the aggregated and the distributed or spatially-aggregated models. While timing differences in the rising and falling limbs of the hydro-

graph were seen, runoff volumes were still adequately represented for a continuous, single snowmelt event, as observed in 2002. However, for a more complex snowmelt season with discontinuous snowmelt events, such as in 2003, the aggregated model was unable to predict timing and runoff volume because topographic effects in incoming shortwave radiation are not effectively represented.

From a conceptual perspective, the combination of deductive and inductive modelling approaches appears to be an appropriate framework for representing and conceptualising landscape heterogeneity in sub-arctic environments. The inductive modelling approach was used to segment the basin, or choose the aggregation level, based on previous understanding of the hydrological response of the various landscape units (i.e. snow-cover area and basin discharge), as well as to conceptualise less well-known processes, such as spring soil water storage dynamics and routing processes. The deductive modelling approach was applied to physically describe and quantify the main hydrological processes such as snow-cover ablation and infiltration into frozen soils.

Calibration was obviously simpler in the aggregated model; however, the greater degrees of freedom in the distributed model allowed for a better description of basin runoff. The fact that minimal calibration was performed to model snow-cover ablation suggested that the EBSM is a simple yet reliable physically-based snowmelt model. This also agrees with the findings of Walter *et al.* (2005), in which better snowmelt simulations, compared with temperature-index models, were obtained using physically-based models with minimal data requirements.

The inclusion of spatially-distributed information clearly improved hydrological prediction, highlighting the importance of incorporating slope and aspect effects on snow accumulation, snowmelt energetics, resulting meltwater fluxes, and runoff contributing area, to reduce input uncertainty. Moreover, the combination of deductive and inductive modelling approaches appears to offer advantages to the top-down or bottom-up approach alone for reducing data, model structure, and parameter uncertainties and for developing regional snowmelt runoff models at small to medium scales in sub-arctic mountainous environments. It should be stressed that it was not the purpose of this study to mimic the shape of the hydrograph or to define an optimum size of the model units, but rather to emphasize that a combined modelling approach can improve model prediction in poorly gauged basins. Therefore, this approach is a credible representation of the system, as it not only describes the snowmelt and discharge well, but also provides a framework that has direct relevance to the physical reality of the system under study.

The presence of a continuous baseflow, the relatively low percentage of the initial SWE that becomes snowmelt runoff, and the role of the organic soil layer in generating fast runoff response at early stages of the snowmelt season, suggest the necessity of improving the conceptual soil moisture balance approach. The new formulation should link groundwater flow with streamflow, improve basin storage options, and adequately account for interflow or subsurface runoff. Further investigations involving the testing of the infiltration into frozen soil equation on slopes, and the evaluation of canopy effects enhancing snowmelt rates and abrupt albedo changes will contribute to the proper definition of model complexity at small to medium scales in northern mountain environments.

**Acknowledgements** The authors would like to acknowledge the assistance of R. Janowicz, G. Carpenter, G. Ford (Yukon Environment), N. Hedstrom, R. Granger (Environment Canada), R. Essery, J. Sicart and D. Bewley (University of Wales), R. Harding and D. Clark (NERC Centre for Ecology and Hydrology), T. Link (University of Idaho), S. McCartney and M. Solohub (University of Saskatchewan) for assistance in taking field observations. Funding for this study was provided by CFCAS, NSERC, CRC, CFI and Environment Canada (Canada), NERC (UK), NOAA OGP (USA). The study is a contribution to the IAHS Decade for Prediction in Ungauged Basins (PUB).

## REFERENCES

- Bewley, D., Pomeroy, J. W. & Essery, R. L. H. (2007) Solar radiation transfer through a sub-arctic shrub canopy. *Arctic, Antarctic, and Alpine Res.* **39**, 365–374.
- Blöschl, G. (1999) Scaling issues in snow hydrology. *Hydrol. Processes* **13**, 2149–2175.
- Blöschl, G. & Sivapalan, M. (1995) Scale issues in hydrological modelling—a review. *Hydrol. Processes* **9**, 251–290.
- Carey, S. K. & Quinton, W. L. (2004) Evaluating snowmelt runoff generation in a discontinuous permafrost catchment using stable isotope, hydrochemical and hydrometric data. *Nordic Hydrol.* **35**, 309–324.
- Carey, S. K. & Quinton, W. L. (2005) Evaluation of runoff generation during summer using hydrometric, stable isotope and hydrochemical methods in a discontinuous permafrost environment. *Hydrol. Processes* **19**, 95–114.
- Carey, S. K. & Woo, M. K. (1998) Snowmelt hydrology of two subarctic slopes, southern Yukon, Canada. *Nordic Hydrol.* **29**, 331–346.
- Carey, S. K. & Woo, M. K. (2000) The role of soil pipes as a slope runoff mechanism, subarctic Yukon, Canada. *J. Hydrol.* **233**, 206–222.
- Carey, S. K. & Woo, M. K. (2001) Spatial variability of hillslope water balance, Wolf Creek basin, subarctic Yukon. *Hydrol. Processes* **15**, 3113–3132.
- Dornes, P. F., Pomeroy, J. W., Pietroniro, A., Carey, S. K. & Quinton, W. L. (2006) The use of inductive and deductive reasoning to model snowmelt runoff from northern mountain catchments. In: *Proc. iEMSs Third Biennial Meeting "Summit on Environmental Modelling and Software"* (Burlington, 9–13 July 2006). International Environmental Modelling and Software Society, VT, USA. <http://www.iemss.org/iemss2006/sessions/all.html>.
- Essery, R. & Pomeroy, J. (2004) Implications of spatial distribution of snow mass and melt rate for snow-cover depletion: theoretical considerations. *Ann. Glaciol.* **38**, 735–774.
- Flügel, W. A. (1995) Delineating hydrological response units (HRUs) by GIS analysis for regional hydrological modelling using PRMS/MMS in the drainage basin of the River Bröl, Germany. *Hydrol. Processes* **9**, 423–436.
- Garnier, B. J. & Ohmura, A. (1970) The evaluation of surface variations in solar radiation income. *Solar Energy* **13**, 21–34.
- Granger, R. J. & Gray, D. M. (1989) Evaporation from natural non-saturated surfaces. *J. Hydrol.* **111**, 21–29.
- Granger, R. J. & Pomeroy, J. W. (1997) Sustainability of the western Canadian boreal forest under changing hydrological conditions, 2. Summer energy and water use. In: *Sustainability of Water Resources under Increasing Uncertainty* (ed. by D. Rosjberg, N. Boutayeb, A. Gustard, Z. Kundzewicz & P. Rasmussen), 243–250. IAHS Publ. 240. IAHS Press, Wallingford, UK.
- Granger, R. J., Pomeroy, J. W. & Essery, R. (2006) Boundary layer growth over snow and soil patches. *Hydrol. Processes* **20**, 943–951.
- Gray, D. M. & Landine, P. G. (1987) Albedo model for shallow Prairie snowcovers. *Can. J. Earth Sci.* **24**, 1760–1768.
- Gray, D. M. & Landine, P. G. (1988) An energy-budget snowmelt model for the Canadian Prairies. *Can. J. Earth Sci.* **25**, 1292–1303.
- Gray, D. M., Toth, B., Zhao, L., Pomeroy, J. W. & Granger, R. J. (2001) Estimation areal snowmelt infiltration into frozen soils. *Hydrol. Processes* **15**, 3095–3111.
- Grayson, R. & Blöschl, G. (2001) Spatial modeling of catchment dynamics. In: *Spatial Patterns in Catchment Hydrology. Observations and Modeling* (ed. by R. Grayson & G. Blöschl), 51–81. Cambridge University Press, Cambridge, UK.
- Lehning, M., Völksch, I., Gustafsson, D., Nguyen, T. A., Stähli, M. & Zappa, M. (2006) ALPINE3D: a detailed model of mountain surface processes and its application to snow hydrology. *Hydrol. Processes* **20**, 2111–2128.
- List, R. J. (1968) *Smithsonian Meteorological Tables* (sixth edn). Smithsonian Inst., Washington DC, USA.
- McCartney, S. E. (2006). Spatial variability of snowmelt water balances in a subarctic catchment. MSc Thesis, University of Saskatchewan, Saskatoon, Saskatchewan, Canada.
- McCartney, S. E., Carey, S. K. & Pomeroy, J. W. (2006) Intra-basin variability of snowmelt water balance calculations in a subarctic catchment. *Hydrol. Processes* **20**, 1001–1016.
- Marks, D., Winstral, A. & Seyfried, M. (2002) Investigation of terrain and forest shelter effects on patterns of snow deposition, snowmelt and runoff over a semi-arid mountain catchment using simulated snow redistribution fields. *Hydrol. Processes* **16**, 3605–3626.
- Pietroniro, A. & Soulis, E. D. (2003) A hydrology modelling framework for the Mackenzie GEWEX programme. *Hydrol. Processes* **17**, 673–676.
- Pomeroy, J. W. & Granger, R. J. (1999) Wolf Creek Research Basin: Hydrology, Ecology, Environment. Environment Canada, Saskatoon, Canada.
- Pomeroy, J. W., Toth, B., Granger, R. J., Hedstrom, N. R. & Essery, R. L. H. (2003) Variation in surface energetics during snowmelt in complex terrain. *J. Hydromet.* **4**, 702–716.
- Pomeroy, J. W., Essery, R. L. H. & Toth, B. (2004) Implications of spatial distributions of snow mass and melt rate for snow-cover depletions: observations in a subarctic mountain catchment. *Ann. Glaciol.* **38**, 195–201.
- Pomeroy, J. W., Bewley, D. S., Essery, R. L. H., Hedstrom, N. R., Link, T., Granger, R. J., Sicart, J. E., Ellis, C. R. & Janowicz, J. R. (2006) Shrub tundra snowmelt. *Hydrol. Processes* **20**, 923–942.
- Pomeroy, J. W., Gray, D. M., Brown, T., Hedstrom, N. R., Quinton, W., Granger, R. J. & Carey, S. K. (2007) Basing process representation and model structure on the evidence of experimental observations. *Hydrol. Processes* **21**, 1241–1247.
- Quinton, W. L. & Gray, D. M. (2001) Toward modelling seasonal thaw and subsurface runoff in arctic tundra environments. In: *Soil-Vegetation-Atmosphere Transfer Schemes and Large-Scale Hydrological Models*. (ed. by H. Dolman, J. Pomeroy, T. Oki & A. Hall), 333–341. IAHS Publ. 270. IAHS Press, Wallingford, UK.
- Quinton, W. L., Shirazi, T., Carey, S. K. & Pomeroy, J. W. (2005) Soil water storage and active-layer development in a sub-alpine tundra hillslope, southern Yukon Territory, Canada. *Permafrost and Periglacial Processes* **16**, 369–382.
- Satterlund, D. R. (1979) An improved equation for estimating longwave radiation from the atmosphere. *Water Resour. Res.* **15**, 1643–1650.
- Sicart, J. E., Pomeroy, J. W., Essery, R. L. H., Hardy, J. E., Link, T. & Marks, D. (2004). A sensitivity study of daytime net radiation during snowmelt to forest canopy and atmospheric conditions. *J. Hydromet.* **5**, 774–784.

- Sivapalan, M., Takeuchi, K., Franks, S. W., Gupta, V. K., Karambiri, H., Lakshmi, V., Liang, X., McDonnell, J. J., Mendiondo, E. M., O'Connell, P. E., Oki, T., Pomeroy, J. W., Schertzer, D., Uhlenbrook, S. & Zehe, E. (2003a) IAHS Decade on Predictions in Ungauged Basins (PUB), 2003–2012: Shaping an exciting future for the hydrological sciences. *Hydrol. Sci. J.* **48**, 857–880.
- Sivapalan, M., Blöschl, G., Lu, Z. & Vertessy, R. (2003b) Downward approach to hydrological prediction. *Hydrol. Processes* **17**, 2101–2111.
- Wagener, T. (2003) Evaluation of catchment models. *Hydrol. Processes* **17**, 3375–3378.
- Walter, M. T., Brooks, E. S., McCool, D. K., King, L. G., Molnau, M. & Boll, J. (2005) Process-based snowmelt modelling: does it require more input data than temperature-index modelling? *J. Hydrol.* **300**, 65–75.
- Zhao, L. & Gray, D. M. (1999) Estimating snowmelt infiltration into frozen soils. *Hydrol. Processes* **15**, 1827–1842.

**Received 25 October 2006; accepted 23 April 2008**